

# Airy-like patterns in heavy ion elastic scattering

R. Anni

*Dipartimento di Fisica dell'Università, Università di Lecce, Lecce, Italia*

*Istituto Nazionale di Fisica Nucleare, Sezione di Lecce, Lecce, Italia*

## Abstract

A semiclassical analysis of an optical potential cross section is presented. The cross section considered is characterized by the appearance of an *Airy-like* pattern. This pattern is similar to that which is present in many cross sections, which fit the recent measurements of light heavy ion elastic scattering, and is considered as a manifestation of a rainbow phenomenon.

The semiclassical analysis shows that, in the case considered, the oscillations arise from the interference between the contributions from two different terms of a multi-reflection expansion of the scattering function, and, therefore, cannot be associated with the rainbow phenomenon.

The elastic differential cross sections of  $^{16}\text{O}+^{16}\text{O}^{1,2}$  and  $^{16}\text{O} + ^{12}\text{C}^{3,4}$ , recently measured at several energies and over wide angular ranges, are characterized by the appearance of structures which are rather well reproduced using optical potentials with deep real and shallow imaginary parts. A shallow imaginary part allows significant contributions from the internal region and this suggests that the gross structures in the angular distribution can be explained as arising from the contributions of trajectories refracted by the deep real potential.

In order to isolate the contributions from these refracted trajectories, the simple decomposition of the scattering amplitude in near- and far-side components<sup>5</sup> is commonly used: because, usually, for strongly absorbing potentials only the near-side component signifi-

cantly contributes to the cross sections, it results rather natural to think that the far-side component should retain the contributions from trajectories penetrating the internal region.

Applying this decomposition to the optical potential scattering amplitude an *Airy-like* pattern often appears in the far-side cross section and this has stimulated the claim that one is observing a *rainbow* phenomenon.

We remember that the meteorological rainbow phenomenon is produced by the scattering of light by the water-droplets of rain and that a simple, scalar, model of the process is provided by the non-relativistic scattering by a spherical well.

The semiclassical limit for scattering by this potential was discussed in detail by Nussenzveig<sup>6,7</sup> in the framework of an exact multi-reflection expansion of the scattering function, named Debye expansion, in which the  $n$ -th term accounts for the contributions of trajectories which are refracted  $n - 1$  times in the internal region.

In this multi-reflection expansion the primary rainbow is associated with the third term, retaining the contribution from trajectories which propagates two-times in the internal region. Mathematically, the rainbow oscillations arise from the coherent superposition of the contributions from two saddle-points, coalescing at the rainbow scattering angle. In a neighborhood of this angle, the use of uniform asymptotic techniques allows one to express the scattering amplitude in term of an Airy function whose maximum replaces the singularity predicted by the non uniform method.

In order to confirm the rainbow nature of the spectacular *Airy-like* pattern observed in some far-side cross sections it seems desirable to look for the two saddle points contributions which, coalescing at the rainbow scattering angle, should produce the Airy maximum.

In the extreme semiclassical limit, these two saddle point contributions should be obtained directly from the exact scattering function  $S_l$ . In this limit the derivative of the argument of  $S_l$ , with respect to the angular momentum  $l$ , is just the classical deflection function, which should show a maximum or a minimum at the rainbow angle. In practical cases, the derivative of  $\arg(S_l)$  presents a more or less marked oscillatory behavior that prevents the treatment of this quantity as a deflection function. Owing to this it is not possible

to obtain the saddle point contributions by simply using the exact  $S_l$ .

The same happens also for the scattering from a spherical well, and the reason is that the link between the scattering angle and the angular momentum must be looked for in each term of the multi-reflection expansion and not in the exact scattering function.

Unfortunately, at present time, there does not exist an exact multi-reflection expansion for scattering by a generic potential equivalent to the Debye expansion for the spherical well potential. However, a non uniform semiclassical method was proposed<sup>8</sup> for potentials with an arbitrary number of turning points in the complex  $r$ -plane, and a uniform semiclassical technique was developed<sup>9</sup> for the cases in which only three turning points give the main contribution. From both these methods one can derive approximate multi-reflection expansions<sup>8,10</sup> in which the different terms have the same physical meaning as the corresponding terms in the exact Debye expansion for the scattering by a spherical well.

In this brief note we present the results obtained by analyzing, with the uniform multi-reflection expansion, the scattering by one optical potential whose far-side cross section exhibits a striking *Airy-like* pattern. The undesired result obtained is that the *Airy-like* pattern does not arise from interference between two saddle points in the same term of the multi-reflection expansion, but from interference between a saddle point from the second term of the expansion, describing trajectories refracted in the internal region, with a contribution from the first term of the expansion, describing trajectories which do not penetrate the internal region. This last contribution is responsible for the *Fraunhofer-like* pattern in the cross section of the first term of the expansion, supporting the conjecture that it must be considered a diffractive contribution.

The optical potential here considered is one of those obtained<sup>4</sup> by fitting the elastic scattering cross section of  $^{16}\text{O} + ^{12}\text{C}$  at  $E_{Lab} = 132$  MeV. This potential has conventional Saxon-Woods form factors with parameters  $V_0 = 282.2$  MeV,  $R_v = 2.818$  fm and  $d_v = .978$  fm, for the real part, and  $W_0 = 13.86$  MeV,  $R_w = 5.689$  fm and  $d_w = .656$  fm, for the imaginary part. The only modification introduced in the optical potential here used, with respect to the original one, is represented by the use for the Coulomb part of a

proper analytical potential, in order to allow the continuation of the quantities needed in a semiclassical analysis outside the real  $r$ -axis. The differences to the cross section values produced by this substitution are completely irrelevant.

In Fig.1 we show the modulus of  $S_l$  and a rough estimate of the derivative of its argument, obtained using the formula  $\Theta(\lambda) = \arg(S_{l+1}) - \arg(S_l)$ , for integer  $l$  values and with  $\lambda = l + \frac{1}{2}$ . The oscillatory behavior of  $\arg(S_l)$ , that in the following we name the quantum deflection function, in the range of  $l$  values around  $l \simeq 23$  cancels the hope of estimating the cross section by applying the saddle point technique starting from the exact  $S_l$ . However the smooth behavior of both  $\Theta(\lambda)$  and  $|S_l|$  for  $l$  values up to about 18 can be considered a signature of the dominance of a classical contribution in this  $l$  range.

This behavior of  $\Theta(\lambda)$  is just the one expected for the deflection function of trajectories refracted in the internal region of an attractive potential, and should produce a saddle point contribution to the far-side cross section.

A rough estimate of this contribution, from the integer  $l$  values up to 18, is shown by the open dots in Fig. 2. It is orders of magnitude smaller than the far-side cross section (medium thickness dashed curve) at forward angles, but increases for increasing angles until it becomes of the same order of magnitude as the far-side cross section in the region in which the oscillations become more marked.

The simplest quantity in which to look for another saddle point contribution, which interfering with the above one could produce the *Airy-like* pattern, is the scattering function of the naive WKB approximation in which the imaginary part of the potential is treated as a perturbation<sup>11</sup>. This quantity has an argument whose derivative with respect to  $\lambda$  coincides with the classical deflection function calculated with only the real part of the potential. In the present case this deflection function has a minimum of about -310.15 degrees, at  $\lambda \simeq 23.56$ , and indicates the existence of the two desired saddle point contributions.

The contributions from the first of these two branches of the deflection function (thin dashed line in Fig. 2) closely follows the open dots, the second (thin continuous line) results larger at forward angles, but not enough to justify the average behavior of the exact far-side

cross section. The interference between the amplitudes of the two contributions was not calculated; in any case it is evident that their sum does not exhibit any classical rainbow singularity, a singularity that the uniform technique should transform in the Airy maximum. Because the minimum of the deflection function is of -310.15 degrees, this singularity is expected at an angle of 49.85 degrees in the contributions to the cross section from trajectories coming from the near-side of the scattering plane.

These difficulties simply reflect the fact that the naive WKB approximation is too rough for a quantitative analysis of the cross section, and this is confirmed by the comparison of the cross section that it predicts (dotted line in Fig. 2) with the exact one (heavy continuous line).

The reason of the failure of the naive WKB approximation must be looked for in the fact that the addition of a small imaginary part to a real potential can dramatically modify the motion of the turning points, as function of the angular momentum.

In Fig. 3 are shown the positions, for integer  $l$  values, of the turning points nearest to the real  $r$  axis (open dots), and of the orbiting points at which two turning points coalesce, for complex  $l$  values in this case. The small dots refer to the complete potential and the large ones to its real part. The squares show the singularities of the potential nearest to the real axis.

The trajectory of the real turning point, for the real potential, is broken into two branches for the complete one: the first terminating in a location near to a singularity of the real part, the second originating near a singularity of the imaginary part. In the following the turning points of these two branches will be indicated with the subscript 3 and 1.

The trajectory described by the turning point, with positive imaginary part and ending in a position near a singularity of the real potential, is not qualitatively modified. In the following this turning point will be referred with the subscript 2.

The addition of the imaginary part modifies the old trajectory with negative imaginary part. The new trajectory starts in a location near to the old one but ends in a location near a singularity of the imaginary potential.

This turning point and the new one, appearing in the first quadrant near a singularity of the imaginary potential, remain far from the real axis and their contributions will be neglected.

Retaining only the contributions from the turning points labeled from 1 to 3 the uniform semiclassical multi-reflection expansion of  $S(\lambda)$  is given by:

$$S_{SC}(\lambda) = \sum_{n=0}^{\infty} S_n(\lambda), \quad (1)$$

where

$$S_0(\lambda) = \frac{\exp(2i\delta_1)}{N(\frac{S_{21}}{\pi})}, \quad (2)$$

and, for  $n \geq 1$ ,

$$S_n(\lambda) = -(-)^n \frac{\exp[2i(nS_{32} + S_{21} + \delta_1)]}{N^{n+1}(\frac{S_{21}}{\pi})}. \quad (3)$$

In the above equations  $\delta_1$  is the complex WKB phase shift for the turning point  $r_1$ ,  $S_{ij}$  is the action integral, in units of  $\hbar$ , between the turning points  $r_i$  and  $r_j$ , and  $N(z)$  is the *barrier penetrability factor* given by:

$$N(z) = \frac{\sqrt{2\pi}}{\Gamma(\frac{1}{2} + z)} \exp(z \ln z - z). \quad (4)$$

As in the Debye expansion, the first term, usually denominated the *barrier* term, retains the contributions from trajectories not penetrating the internal region, while the  $n$ -th term retains the contributions from trajectories refracted  $n$  times in the internal region with  $n - 1$  reflections at the turning point  $r_2$ .

The modulus and the quantum deflection function of the first two terms of the expansion are shown in Fig. 4. The modulus of the second term (thick dashed line) is much larger than that of the first (thick continuous line) for small  $l$  values, but it decreases while the other increases, until they become equal at  $l \simeq 21$ . For higher  $l$  value the modulus of the first term rapidly increases while that of the second even more rapidly decreases.

The quantum deflection function of the first term (medium continuous line) has the typical behavior, apart from a small neighborhood of the grazing angular momentum, of the

deflection function of trajectories reflected at the surface of a spherical region, in presence of an external small Coulomb field.

The quantum deflection function of the second term (medium dashed line) closely follows the classical deflection function (dotted line) for  $l$ -values smaller than about 20; for higher values of  $l$  it shows a rainbow behavior, less deep and more large than that predicted by classical mechanics. The very small value of the modulus of the scattering function suggests that the saddle point contribution from the branch of the quantum deflection function to the right of the rainbow angular momentum should result completely negligible.

The thin curves represent the cubic spline interpolations, of the integer  $l$  values, of the modulus and the quantum deflection function of the sum of the first two terms of the expansion. These curves are in very good agreement with the dots representing the corresponding exact quantities and provide a simple explanation of the origin of the irregular behavior of the exact quantum deflection function, as arising from the interference between the contributions of two simpler component scattering functions.

The semiclassical cross section, and its near- and far-side components, obtained using in the partial wave expansion the first two terms of the multi-reflection expansion, are shown in panel (a) of Fig. 5. The differences between these quantities and the corresponding exact ones cannot be appreciated within the scale and the thickness used for the curves.

In panel (b) the complete semiclassical cross section is shown together with the separate cross sections of the first two terms of the expansion. The cross section of the first term is characterized by the appearance, at forward angles, of a *Fraunhofer-like* oscillatory pattern, while no *Airy-like* oscillatory pattern is present in that of the second term. The *Airy-like* oscillatory pattern appears only in the complete cross section and arises from the interference between the scattering amplitudes of the two terms.

The near- and far-side decompositions of the cross section of the first and the second term of the expansion are shown in panels (c) and (d), respectively. With the exclusion of the extreme backward scattering angles the cross section of the second term of the expansion is completely far-side and results in very good agreement with the dots that represent the

saddle point contribution to the cross section previously estimated using the exact scattering function.

The *Fraunhofer-like* oscillatory behavior of the first term of the expansion arises from the interference between a near-side and a far-side contribution. It is just the interference between the far-side contributions of the first two terms which is responsible for the *Airy-like* pattern appearing in the far-side component of the complete cross section.

Previous analyses of similar decompositions<sup>10</sup> have shown that the far-side component of the *barrier* term of the expansion retains the contribution from generalized diffracted trajectories. In the uniform semiclassical approximation for the *barrier* scattering function, this contribution should, mathematically, derive from the Sommerfeld pole (or if one likes: the barrier top resonance<sup>12</sup>) located near to the real  $\lambda$ -axis, at the  $\lambda_0$  value for which  $S_{21}(\lambda_0) = -\frac{\pi}{2}$ .

The correctness of this interpretation can only be proved by the direct numerical calculation of the location and of the residue of this pole. In any case, the analysis of the cross section here considered shows that the oscillations in the far-side cross section arise from the interference of contributions from different terms of the multi-reflection expansion. From this it follows that (if one agrees to reserve the *rainbow* denomination to the phenomena having the same justification of the phenomenon observed in meteorology) the use of the rainbow terminology for these oscillations should be avoided.

Irrespective of the nature of the other contribution, and on the denomination of the interference pattern, the present analysis confirms that one of these two contributions is a saddle point one, and that it is associated with trajectories which more or less deeply penetrate the internal region and give important contributions to the optical potential cross section.



## REFERENCES

1. Dao T. Khoa, W. von Oertzen, H. G. Bohlen, and F. Nuoffer, Nucl. Phys. **A672** 387 (2000).
2. M. P. Nicoli, F. Haas, S. Szilner, Z. Basrak, A. Morsad, G. R. Satchler, and M. E. Brandan, Phys. Rev. C **61** 034609 (2000).
3. M. P. Nicoli, F. Haas, R. M. Freeman, N. Aissaoui, C. Beck, A. Elanique, R. Nouicer, S. Szilner, Z. Basrak, A. Morsad, M. E. Brandan, and G. R. Satchler, Phys. Rev. C **60** 064608 (2000).
4. A. A. Ogloblin, Yu. A. Glukhov, W. H. Trzaska, A. S. Dem'yanova, S. A. Goncharov, R. Julin, S. V. Klebnikov, M. Mutterer, M. V. Rozhkov, V. P. Rudakov, G. P. Tiorin, Dao T. Khoa, and G. R. Satchler, Phys. Rev. C **62** 044601 (2000).
5. R. C. Fuller, Phys. Rev. C **12** 1561 (1975).
6. H. M. Nussenzweig, J. Math. Phys. **10** 82 (1969).
7. H. M. Nussenzweig, J. Math. Phys. **10** 125 (1969).
8. J. Knoll and R. Schaeffer, Ann. Phys. (N.Y.) **97** 307 (1976).
9. D. Brink and N. Takigawa, Nucl. Phys. **A279** 159 (1977).
10. R. Anni and L. Renna, Nuovo Cimento A **42** 311 (1981).
11. R. Broglia, S. Landowne, R. A. Malfliet, V. Rostokin and Aa. Winther, Phys. Rep. C **11** 1 (1974).
12. W. A. Friedman and C .J. Goebel, Ann. Phys. (N.Y.) **104** 145 (1977).

## FIGURES

Fig. 1. Modulus (open dots) and derivative of the argument (full dots) of the scattering function. The thin curves show the cubic spline interpolation of the dots.

Fig. 2. Cross section (heavy thick line), near- and far-side components (medium continuous and dashed lines), together with the naive WKB cross section (dotted line) and the saddle point contribution from the two far-side branches of the WKB deflection function (thin continuous and dashed lines). The dots show the saddle point contribution estimated using the exact scattering function.

Fig. 3. Turning points in the complex  $r$ -plane (open dots) and orbiting points (full dots) for the complete potential (small) and for only the real part (large). The squares indicate the singularities of the potential.

Fig. 4. Modulus and deflection function (heavy and medium thickness lines) of the first and second terms (continuous and dashed lines) of the multi-reflection expansion. The thin lines show the same quantities for the sum of the two terms. The the dots are from Fig. 1, and the dotted line shows the classical deflection function of the real potential.

Fig. 5. (a) near- and far-side decomposition (continuous and dashed lines) of the semiclassical cross section (thick line); (b) cross section of the first and second terms (continuous and dashed lines) of the multi-reflection expansion and of their sum (thick line); (c) near- and far-side decomposition (continuous and dashed lines) of the cross section of the first term of the expansion (thick line); (d) the same as (c) for the second term of the expansion.

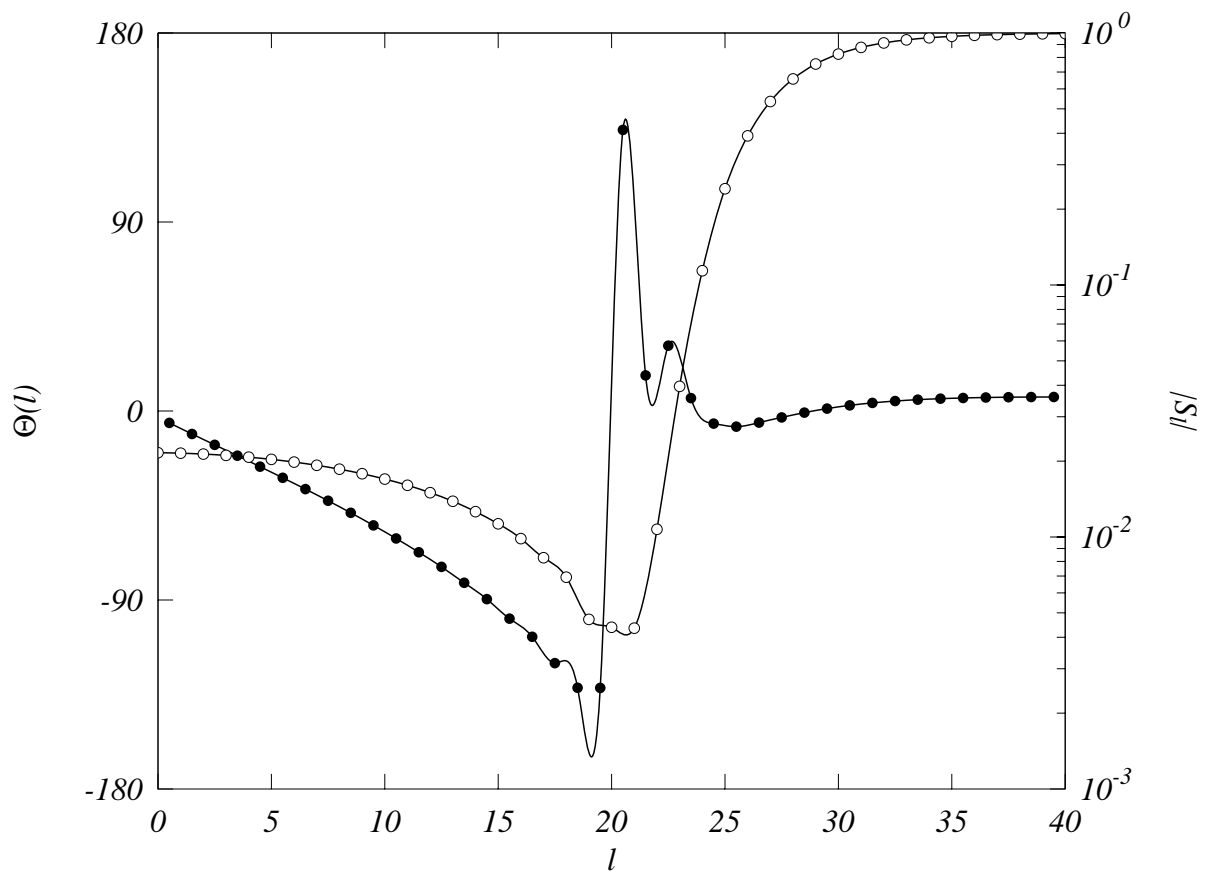


FIG. 1

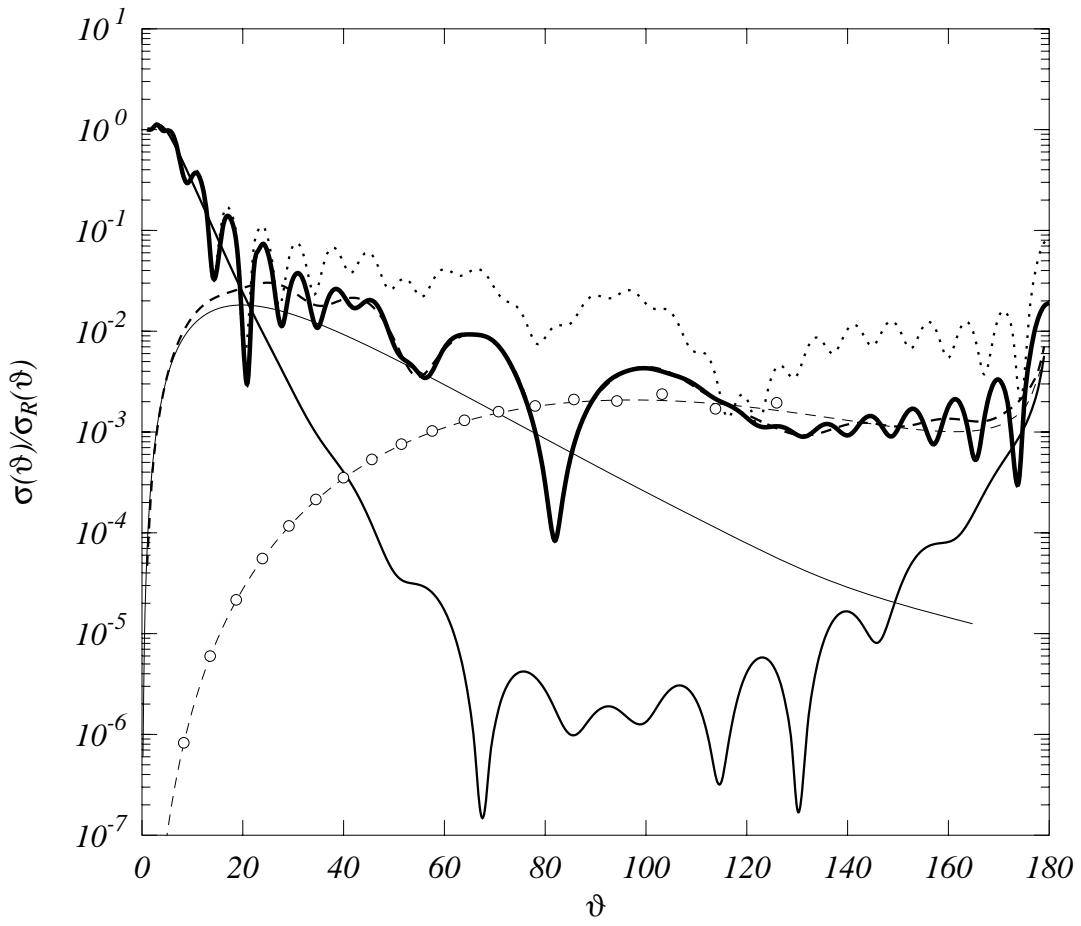


FIG. 2

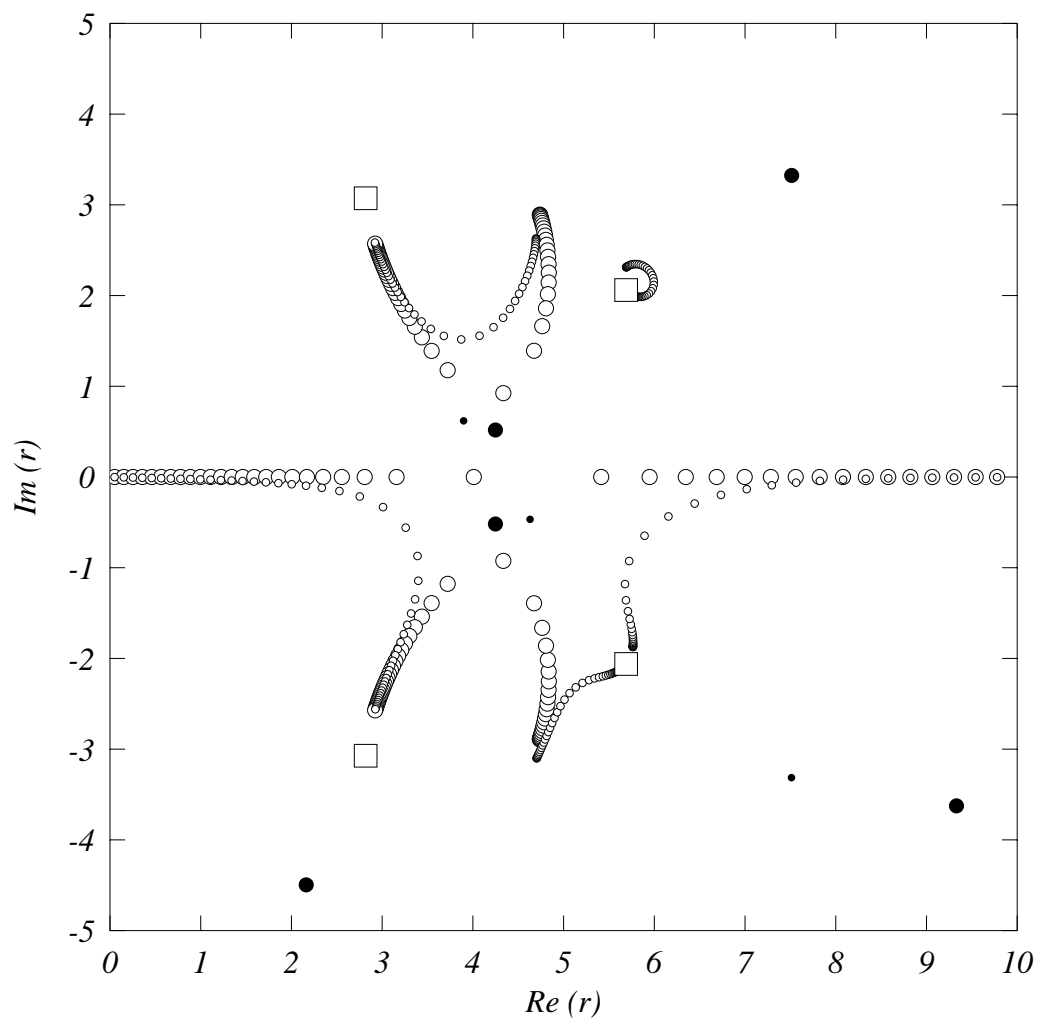


FIG. 3

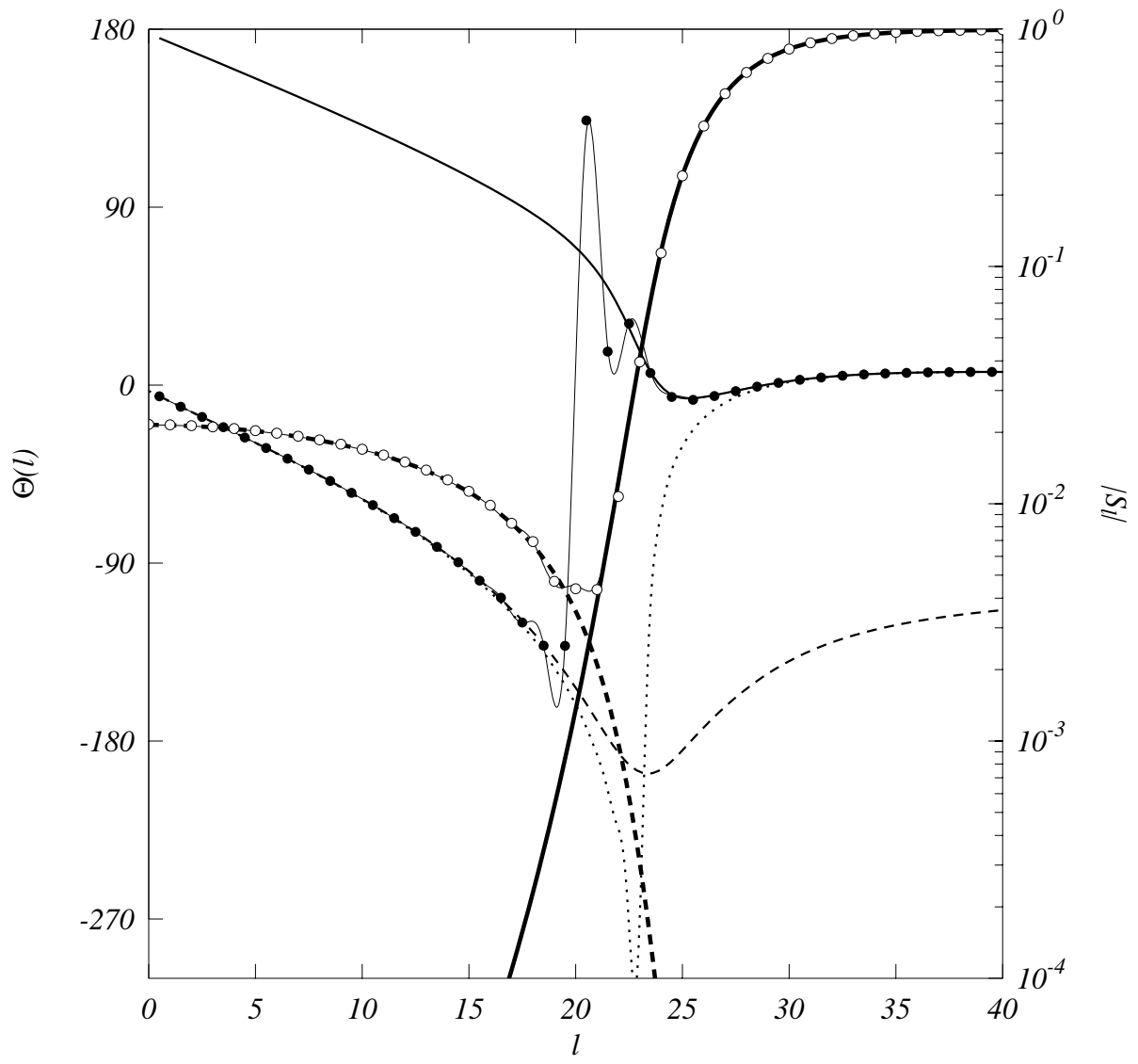


FIG. 4

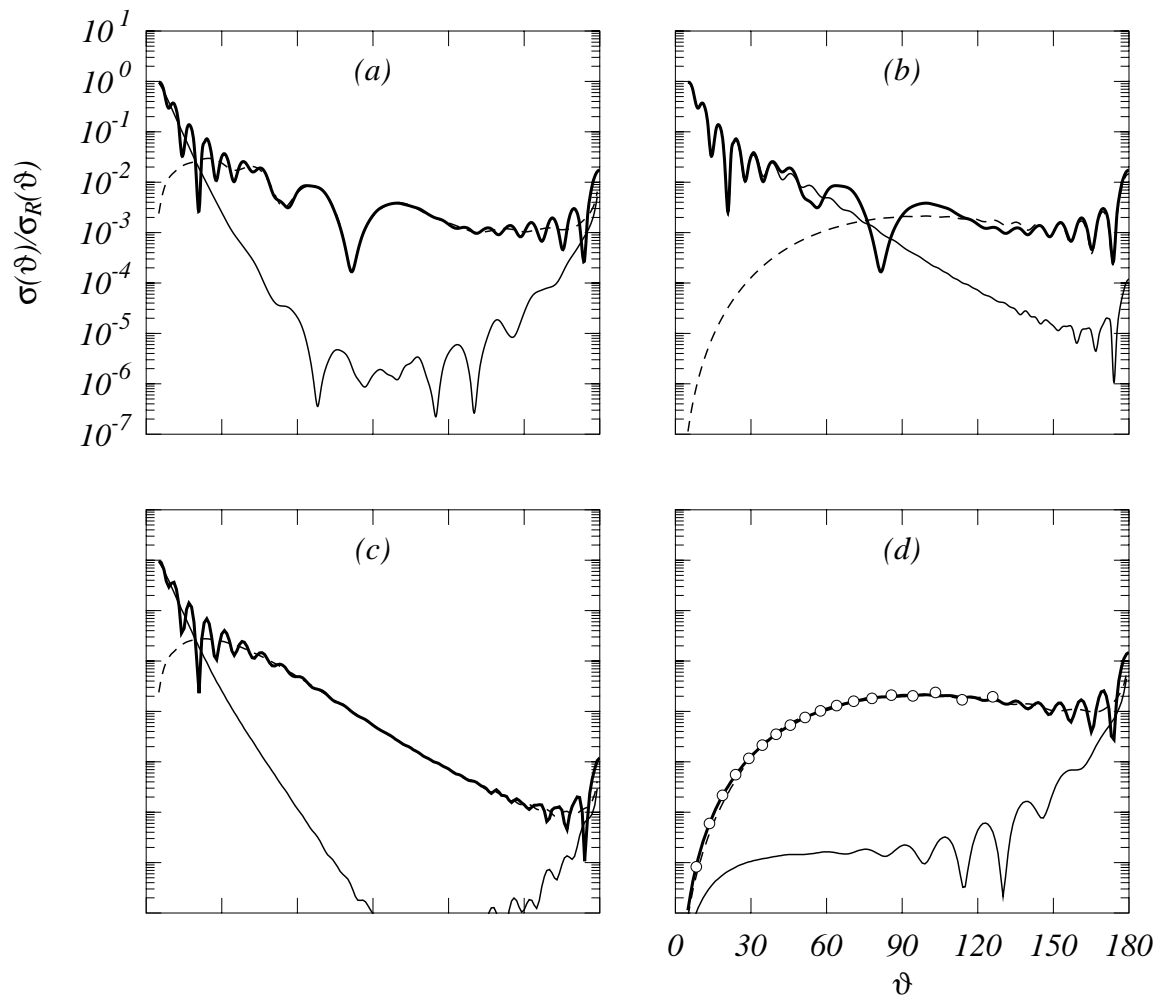


FIG. 5